TÜBİTAK

Turkish Journal of Chemistry

http://journals.tubitak.gov.tr/chem/

Research Article

Turk J Chem
(2017) 41: 99 – 115

doi:10.3906/kim-1603-82

Sonochemical degradation of Basic Red 29 in aqueous media

Zineb BOUTAMINE[1], **Slimane MEROUANI**[1,2,*], **Oualid HAMDAOUI**[1]
[1]Laboratory of Environmental Engineering, Department of Process Engineering, Faculty of Engineering, Badji Mokhtar-Annaba University, Annaba, Algeria
[2]Laboratory of Environmental Process Engineering, Department of Chemical Engineering, Faculty of Process Engineering, University of Constantine 3, Constantine, Algeria

Received: 19.03.2016 • **Accepted/Published Online:** 31.07.2016 • **Final Version:** 22.02.2017

Abstract: In this work, the degradation of Basic Red 29 (BR29), an azo dye, was investigated using a high-frequency ultrasonic reactor (300 kHz). The influence of several parameters such as initial substrate concentration (5–200 mg L^{-1}), pH (3–10.1), ultrasonic power (20–80 W), and nature of the dissolved gas (Ar, air, and N_2) on the degradation of BR29 was assessed. Additionally, the impact of natural matrices (seawater and natural and river waters) on the degradation rate of BR29 was clarified. Degradation experiments with radical scavengers, tert-butyl alcohol and glucose, showed that BR29 degraded mainly through $HO^{\bullet}$ radical attack at the gas/liquid interface of the cavitation bubbles. The degradation of the dye was strongly sensitive to the operational conditions. The natural matrices enhanced the degradation of the dye. Ultrasonic mineralization and oxidation of the dye solution was significantly enhanced by addition of a low quantity of Fe^{2+} (15 mg L^{-1}).

Key words: Ultrasonic degradation, Basic Red 29, $HO^{\bullet}$ radical, natural matrices, mineralization

1. Introduction

The textile dyeing industry consumes large quantities of water and produces large volumes of wastewater from different steps in the dyeing and finishing processes.[1] Wastewater from printing and dyeing units is often rich in color, containing residues of reactive dyes and chemicals, such as complex components, with high chemical oxygen demand (COD) and biochemical oxygen demand (BOD) concentrations as well as more hard-degradation materials.[1] The toxic effects of dyestuffs from industrial establishments on the general public are widely accepted. Discharged wastewater from the textile industry under uncontrolled and unsuitable conditions is causing significant environmental problems. The importance of pollution control and treatment is undoubtedly a key factor in the human future. If a textile mill discharges wastewater into the local environment without any treatment, it will have a serious impact on natural water bodies and land in the surrounding area. High values of COD and BOD_5, the presence of particulate matter and sediments, and oil and grease in the effluent cause depletion of dissolved oxygen, which has an adverse effect on the aquatic ecological system.[2,3] Azo dyes are substances commonly used in textile, cosmetic, pharmaceutical, pulp and paper, food, and other industries and are characterized by the –N=N– group bearing aromatic rings.[4] Their production is more than 1×10^6 t/year in the world, making them the largest group of synthetic colorants.[3] During dyeing processes, about 10%–25% of this huge amount of azo dyes ends up in wastewaters.[4] The presence of these chemicals in wastewater presents

*Correspondence: s.merouani@yahoo.fr

a potential human health risk as some of them have been shown to be carcinogenic.[5,6] Thus, efficient treatment of dye wastewater before its discharge is an international requirement.

In the past several decades, many techniques have been developed to find an economic way to treat textile dyeing wastewater, including physicochemical (flotation, coagulation-flocculation-sedimentation, adsorption, and membrane separation processes), biological (aerobic and anaerobic methods), and other technologies.[7] However, physicochemical treatments are separation techniques that only transfer the pollutants from one phase to another phase. Biological methods present the disadvantages of low biotransformation kinetics, the formation of sludge, and nonresistance to some refractory dyes.[8−10] Recent developments in the domain of wastewater treatment have led to an improvement in oxidative degradation procedures for recalcitrant organic compounds dissolved or dispersed in aquatic media, in applying advanced oxidation processes (AOPs).[11−13]

AOPs can be broadly defined as aqueous phase oxidation methods based on the intermediacy of highly reactive species such as hydroxyl radicals ($HO^{\bullet}$). Thanks to its high standard reduction potential of 2.8 V vs. NHE,[14] these radicals are able to oxidize, with rate constants usually on the order of 10^6 to 10^9 mol L^{-1} s^{-1},[15] and mineralize partially or totally almost all organic compounds to carbon dioxide and water. The most commonly applied AOPs range from Fenton's oxidation and ozone to ultraviolet (UV) light, photocatalysis, UV/H_2O_2, and a combination of these processes.[12,13,16]

A new way for generating hydroxyl radicals is the application of high-power ultrasound.[17,18] The passage of ultrasound irradiation with frequency in the range of 20–1000 kHz through liquid induces the so-called acoustic cavitation, which is the formation, growth, and implosive collapse of microbubbles containing dissolved gases and water vapor.[19] Practically, all chemical and physical effects of ultrasound in an aqueous solution originate from this phenomenon.[19] The rapid collapse (several nano- or microseconds) of cavitation bubbles is nearly adiabatic, rendering each individual bubble a microreactor, inside which temperatures of the order of 5000 K and pressures of about 1000 atm have been shown to exist.[20] As a result, water vapor entrapped inside a bubble is dissociated into $H^{\bullet}$ and $HO^{\bullet}$ radicals, and with other species present, various other reactive entities such as $HO_2^{\bullet}$ and O may form.[21,22] Parallel reaction pathways exist where volatile solutes may evaporate into the bubble and be pyrolyzed by the high core temperatures.[23] The radical species produced can recombine, react with other gaseous species present in the gas phase, or diffuse into the bulk liquid surrounding the bubble.[23] Reactions involving free radicals can occur within the collapsing bubble, at the liquid interface, and in the surrounding liquid.[23] Accordingly, the sonochemical degradation of an organic compound can occur in gas-phase pyrolysis and oxidation for volatile substrates and by reaction with $HO^{\bullet}$ radicals at the bubble/liquid interface and in the aqueous phase for nonvolatile substrates.[24] In the absence of solutes in the solution, the primary active species of sonolysis mostly recombine at the bubble solution interface to form hydrogen peroxide (Eqs. (1) and (2)).[24] Cavitation bubbles due to the very high temperatures generated at the final stages of bubble collapse emit light that is known as sonoluminescence.[25]

$$2HO^{\bullet} \rightarrow H_2O_2 \quad k_1 = 5.5 \times 10^9 M^{-1} s^{-1} \tag{1}$$

$$2HO_2^{\bullet} \rightarrow H_2O_2 + O_2 \quad k_2 = 8.3 \times 10^5 M^{-1} s^{-1} \tag{2}$$

In spite of the frequent use of ultrasound for the degradation of organic compounds, no data have been given for the degradation of Basic Red 29 (BR29) azo dye using high-frequency ultrasound. BR29 can be regarded as a model substrate that represents all kinds of dyes because all organic dyes are characterized by a chromophore

group and at least one aromatic derivative ring. The chromophore group has an absorption band in the visible region and the aromatic derivative range band is located in the UV region. These two characteristic bands are very reactive toward hydroxyl radical attack.[26] Consequently, the purpose of this research is to assess the degradation of BR29, a mono azo dye, by application of high-frequency ultrasonic waves (300 kHz). This frequency was reputed to be the best for the degradation of nonvolatile organic contaminants.[27] The influence of several operating parameters (initial dye concentration, pH, power, and the nature of dissolved gas) on the degradation rate was clarified. Additionally, to evaluate the potential of ultrasound at 300 kHz towards the treatment of real wastewaters, the degradation of the dye was assessed in complex matrices such as seawater and natural and river waters. Finally, the mineralization and oxidation of the dye solution was examined and an improvement method was proposed and proven.

1.1. Single bubble sonochemistry model

For proving the formation of free radicals during the collapse of acoustic cavitation bubbles in liquid water and hence estimating their concentrations, a mathematical algorithm based on a single bubble sonochemistry model was employed. This model, which combines a dynamic equation for an osculating bubble in aerated water under the action of an ultrasound wave with chemical kinetics consisting of 73 reversible chemical reactions occurring in the bubble during its strong collapse, was well described in our previous reports.[28–31]

2. Results and discussion

2.1. UV-Vis spectra during the ultrasonic treatment of BR29

Figure 1 shows the evolution of the UV-Vis spectrum recorded prior to and during the ultrasonic treatment at 300 kHz and 80 W of an aqueous solution of BR29 (initial concentration: 30 mg L^{-1}) at natural pH. As seen, the initial BR29 solution has two characteristic absorption bands: the first appears in the visible region, with λ_{max} = 511 nm, is that of the chromophoric group of the dye, and the second is in the UV region, with λ_{max} = 285 nm (absorption of the derivative aromatic rings). As illustrated in Figure 1, the absorption peak of BR29 in the visible and UV bands declined with increasing irradiation time until no peaks were further observed after 120 min. This implies the cleavage of the N–N and/or C–N bonds of the dye molecule as well as the destruction of aromatic rings. Because of the hydrophilic and nonvolatile character of BR29 (solubility in water: $\sim$ 50 g L^{-1}), $HO^{\bullet}$ attack on BR29 at the exterior of the cavitation bubble is the main suspected pathway of dye degradation. The destruction of the dye is accompanied by the formation of a new peak at 205 nm, which represents the absorption of the degradation by-products formed during the son-oxidative process as well as nitrous and nitric acids. The intensity of this peak increased with increasing sonication time (Figure 1), indicating the increase of the by-products and nitrous and nitric acids concentration. To avoid confliction between BR29 and its by-products in the UV region, the degradation of the dye during the reaction period was assessed at 551 nm, at which only BR29 absorbs.

2.2. Reactivity zone and sono-oxidation mechanism

In sonochemical treatment, knowledge of the exact zone in which the degradation of the pollutant takes place and the reactive species involved in this process is very important in interpreting the effect of all parameters on the degradation rate of the contaminant. Our initial focus was thus the characterization of the substrate sonolysis by determining the local zone and the species involved into the sonodegradation process of the dye.

For this aim, sonolytic experiments (300 kHz, 80 W, and 30 mg L^{-1} BR29) were conducted in the presence of two $HO^{\bullet}$ radical scavengers, tert-butyl alcohol as a scavenger in the gas phase, and glucose as a scavenger in the bulk solution.[32–34]

Figure 2 shows the effects of tert-butyl alcohol and glucose, at various concentrations, on the degradation rate of BR29. As seen from this figure, the presence of tert-butyl alcohol considerably quenches the destruction of the dye, particularly at high alcohol levels. Tert-butyl alcohol is a highly volatile compound that penetrates easily into the bubble during its expansion phase and degrades at the later stage of the bubble's collapse via a free-radical pyrolysis mechanism in which the alcohol consumes $HO^{\bullet}$ radicals and prevents their accumulation at the bubble interface.[32] Hence, tert-butyl alcohol experiments confirm (i) the nonpyrolytic degradation of BR29 inside the bubble and (ii) the $HO^{\bullet}$ attack of the dye molecules at the outside of the bubble. More information about the exact degradation zone was obtained by the addition of glucose. Glucose is more highly water-soluble (solubility: 661 g L^{-1}) than the target molecule (BR29). It degrades mainly through the reaction with $HO^{\bullet}$ radical in the bulk of the solution.[34] As can be seen from Figure 2, the addition of glucose with high concentration levels has practically no effect on the sonolytic degradation of the dye, signifying that BR29 degradation with $HO^{\bullet}$ radical takes place mainly at the surface of the collapsing bubble, far from the reactivity zone of glucose (the bulk solution).

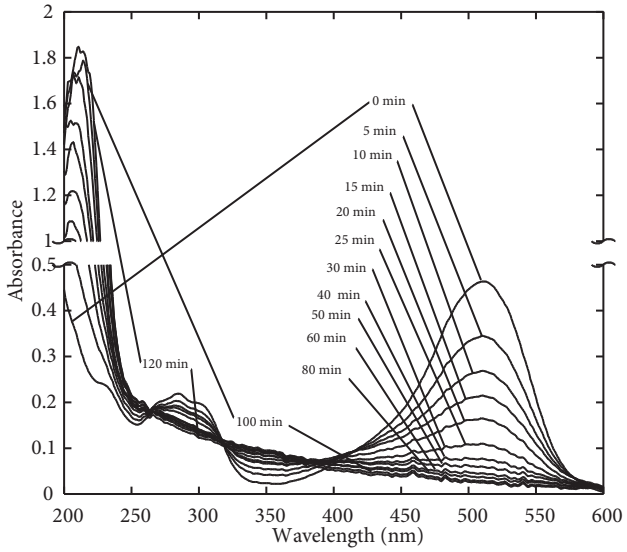

Figure 1. Temporal variation of the UV-Vis spectra of BR29 solution upon ultrasonic action (conditions – volume: 300 mL, initial BR29 concentration (C_0): 30 mg L^{-1}, temperature: 25 ± 2 °C, pH ∼5.6, frequency: 300 kHz, power: 80 W).

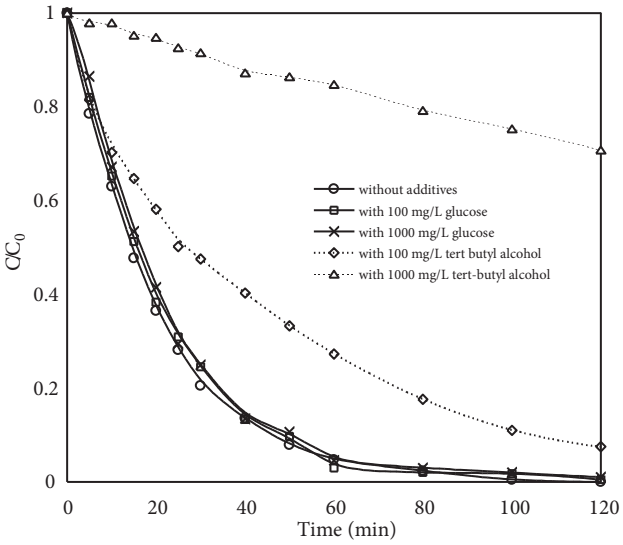

Figure 2. Effect of additions of radical scavengers, tert-butyl alcohol and glucose, at 100 and 1000 mg L^{-1} on the sonochemical degradation of BR29 (conditions – volume: 300 mL, initial BR29 concentration (C_0): 30 mg L^{-1}, temperature: 25 ± 2 °C, pH ∼5.6, frequency: 300 kHz, power: 80 W).

2.3. Experimental and numerical evidence of $HO^{\bullet}$ radical formation at 300 kHz

The formation of $HO^{\bullet}$ radical during water sonolysis at low frequency (50 kHz) was experimentally evidenced by Makino et al.[21] using ESR spin trapping. It is of interest to verify whether our sonochemical reactor operating at high frequency (300 kHz) is able to produce radicals in sufficient quantity to degrade pollutants. Thus, a

characterization of the sonochemical reactor, in terms of radical production, is necessary. In our study, KI dosimetry was used to assess the hydroxyl radical formation by photometrically monitoring the oxidation of iodide ions (I^-) into triiodide ions (I_3^-). To this end, 300 mL of KI aqueous solution (0.1 M) was irradiated at 300 kHz and 80 W. I^- ions are oxidized to I_3^- by means of $HO^\bullet$ radicals according to the reactions presented in Eqs. (3)–(5).[35,36] The amount of the generated I_3^- ions was quantified spectrophotometrically at 352 nm (extinction coefficient = 26000 L mol^{-1} cm^{-1}). The number of hydroxyl radicals formed during sonication was quantified by observing the amount of I_3^- produced.

$$^\bullet OH + I^- \rightarrow I + OH^- \tag{3}$$

$$2I \rightarrow I_2 \tag{4}$$

$$I_2 + I^- \rightarrow I_3^- \tag{5}$$

The plot of triiodide concentration (μM) against time (min) for 1 h of sonolysis give a linear relationship and the rate of I_3^- formation was calculated as 4.38 μM min^{-1}. According to the stoichiometry of the reaction, the production rate of $HO^\bullet$ should be twofold that of I_3^-, i.e. 8.76 μM min^{-1}.

The formation of $HO^\bullet$ radical during water sonolysis at 300 kHz was also evidenced theoretically using the model described for single bubble sonochemistry. Figures 3a and 3b show the calculated results of the liquid pressure and the bubble radius as a function of time for four acoustic cycles ($\sim$13.5 μs) under 300 kHz and 80 W. The ambient bubble radius is 5 μm because it is the typical value of active bubbles at around 300 kHz.[37–39] It is seen that the bubble initially expands during the rarefaction phase of the ultrasound wave, reaches a maximum ($\sim$23 μm) at the beginning of the compression phase, and then strongly collapses during the compression phase and expands again during the subsequent rarefaction phase of the ultrasound wave. This behavior was experimentally reported for sonoluminescing acoustic bubbles.[25] The stronger bubble implosion is clearly reflected by the high speed of the bubble wall ($\sim$250 m s^{-1} at the final stage of bubble collapse) during the compression phase, as can be seen from Figure 3c. These stronger collapses generate extremely higher conditions inside the bubble. Indeed, the bubble's internal pressure and temperature may increase up to 2200 atm and 5100 K at the end of each bubble collapse, as can be observed in Figures 3d and 3e. Under such conditions, combustion reactions occur in the bubble on a time scale of $\sim$0.03 μs and many products are formed by H_2O and O_2 dissociation and their associate reactions, as can be seen in Figure 4, which is an enlarged view of the numerical simulation results of the internal bubble chemistry at the end of the first collapse ($\sim$3.136 μs). The principal vertical axis of this figure is in logarithmic scale. From this figure, it is clearly seen that among several formed oxidants products, the $HO^\bullet$ radical is the first and the dominant powerful oxidant of the combustion reaction in the bubble. It attained its upper concentration (5.208 $\times$ 10^{-15} mol) at the end of the bubble collapse (at R_{min}), followed by almost constant production as the bubble temperature decreased suddenly after that instant. The $HO^\bullet$ radical constitutes $\sim$30% of the total amount of the oxidants formed in the bubble. The number of active bubbles formed in the reacting medium may be predicted using the following equation:[31]

$$N = \frac{r_{H_2O_2}}{n_{H_2O_2} + 0.5(n_{^\bullet OH} + n_{HO_2^\bullet})} \tag{6}$$

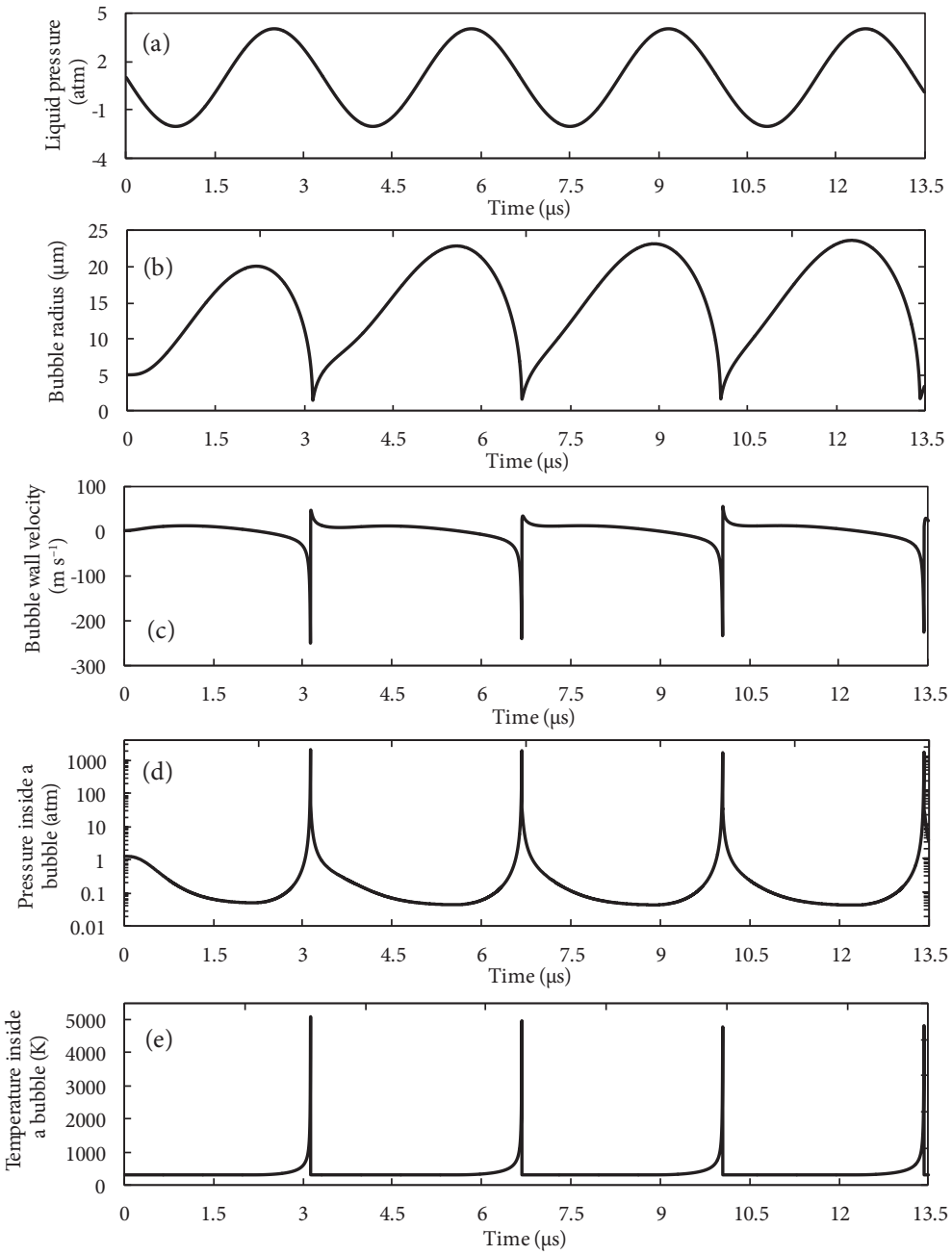

Figure 3. The calculated results of the liquid pressure (a), the bubble radius (b), the bubble wall velocity (c), the pressure inside a bubble (d), and the temperature inside a bubble (e) as a function of time for 4 acoustic periods at 300 kHz (conditions – ambient bubble radius: 5 μm, power: 80 W, liquid temperature: 25 °C). The liquid pressure in (a) is the sum of the acoustic pressure and the static pressure (1 atm). The vertical axis in (d) is in logarithmic scale.

where $r_{H_2O_2}$ is the production rate of H_2O_2 in pure water (determined analytically as 5.15 μM min^{-1} using the iodometric method) and the entities $n_{H_2O_2}$, $n_{\bullet OH}$, and $n_{HO_2\bullet}$ are the number of moles of H_2O_2, $HO^\bullet$, and $HO_2^\bullet$ released by each bubble at the end of the first collapse (obtained from Figure 4). At 300 kHz and 80 W, the number of active bubbles was predicted to be 3.23 $\times$ 10^7 s^{-1} L^{-1}, which yields an overall production

rate of $HO^{\bullet}$ (number of bubbles multiplied by the single bubble yield) of 10.1 μM min^{-1}. As can be observed, the predicted production rate of $HO^{\bullet}$ (10.1 μM min^{-1}) is in the same order of magnitude as that determined using KI dosimetry (8.76 μM min^{-1}). Consequently, the numerical simulations confirmed the formation of hydroxyl radical during sonolysis at 300 kHz.

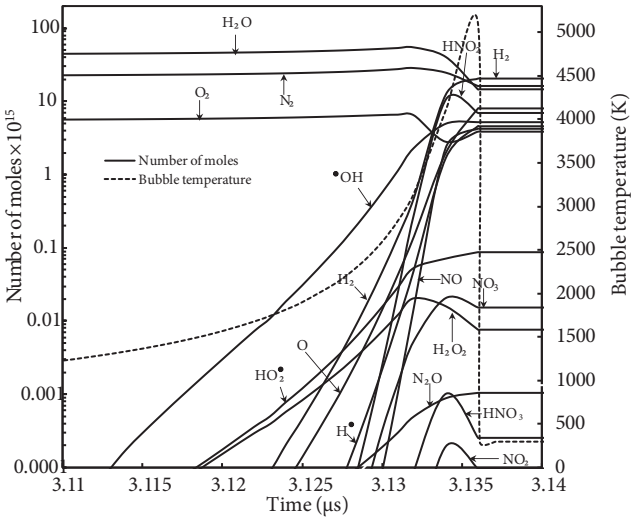

Figure 4. Evolution of the reaction system inside a bubble as a function of time at around the end of the first bubble collapse, for the same conditions as in Figure 3. The principal vertical axis is in logarithmic scale. The horizontal axis is only for about 0.03 μs. The numerical simulation of chemical reactions was conducted for a bubble initially composed of air and water vapor.

2.4. Effect of initial BR29 concentration

The effect of initial concentration of BR29 on its sonolytic degradation was studied in the concentration range of 5–200 mg L^{-1} under 300 kHz and 80 W. Whatever the initial concentration of the dye, sonolysis was able to remove BR29 as indicated in Figure 5a. The removal amount of the pollutant increased significantly with increasing dye concentration (Figure 5b), i.e. 4.3- and 11.7-fold increase was recorded when initial BR29 concentration increased from 5 to, respectively, 30 and 100 mg L^{-1}. On the other hand, even if the concentration profiles of BR29 decreased exponentially with time (Figure 5a), the sonolytic degradation rate of BR29 cannot be described with the first-order kinetics law. The initial degradation rate increased significantly with increasing initial concentration, but a linear relationship was not observed, as shown in Figure 6. A heterogeneous kinetics model based on the Langmuir equation (Eq. (7)) was applied to fit the experimental data.[40] This model, which was largely used for describing the sonochemical degradation rates, assumes automatically that reactions take place at the surface of the cavitation bubble.[41–43]

$$r = \frac{kKC_0}{1 + KC_0} \tag{7}$$

Here, r is the initial degradation rate (mg L^{-1} min^{-1}), k is the pseudo rate constant (mg L^{-1}), K is the equilibrium constant (L mg^{-1}), and C_0 (mg L^{-1}) is the initial concentration of BR29. The model parameters (k = 5.5272 mg L^{-1} min^{-1} and K = 0.0102 L mg^{-1}) were determined by a nonlinear curve fitting method using KaleidaGraph software and the corresponding theoretical curve was superimposed on the experimental

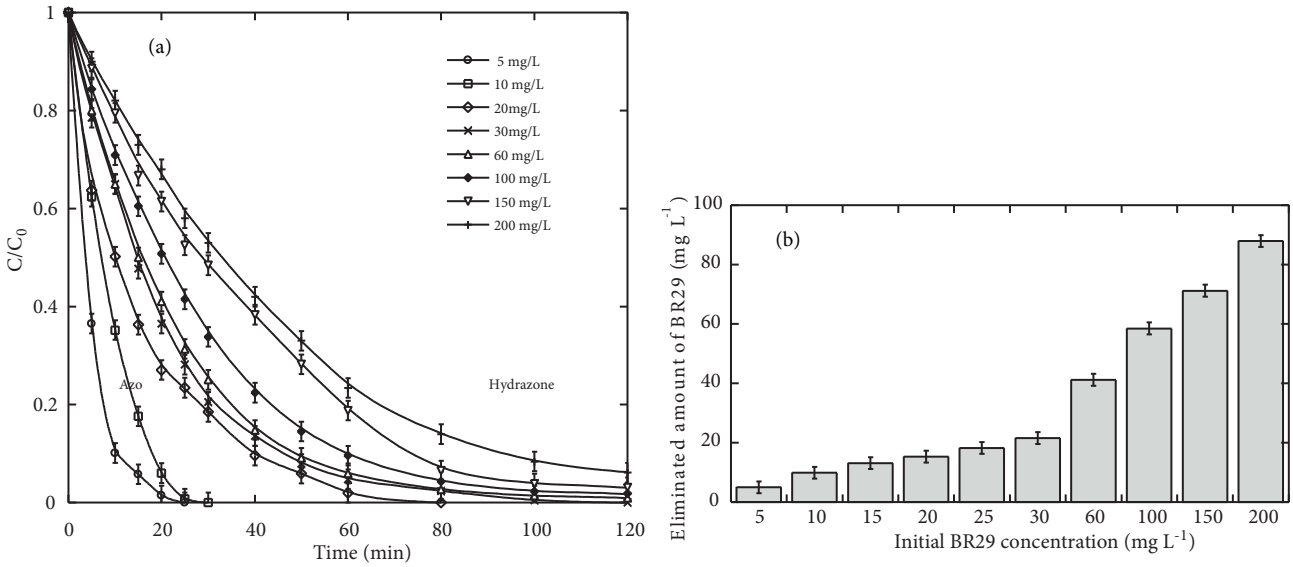

Figure 5. Degradation kinetics (a) and eliminated amount of BR29 (b) for various initial dye concentrations during ultrasonic treatment of BR29 aerated solutions (conditions – volume: 300 mL, initial dye concentration (C_0): 5–200 mg L^{-1}, temperature: 25 ± 2 °C, pH ∼5.6, frequency: 300 kHz, power: 80 W). The eliminated amount was calculated after 25 min of treatment.

data points (Figure 6). It is clearly seen that the Langmuir kinetic model perfectly described the sonolytic degradation rate of BR29, signifying that the BR29 degradation process is a predominately interfacial event. Based on this result, it can be concluded that the degradation of the dye depends on both the substrate and hydroxyl radical concentrations at the bubble/solution interface. At low concentrations of BR29, a fraction of the $HO^{\bullet}$ radicals formed during sonolysis may attack BR29 molecules and the remaining $HO^{\bullet}$ radicals recombine to yield H_2O_2 (Eq. (1)). However, as the concentration of BR29 is increased, the fraction of $HO^{\bullet}$ radicals that undergo recombination would decrease and be involved in the degradation process and hence the degradation rate would increase. This was reported by several studies and was supported by the fact that H_2O_2 production rates were decreased with the increase in pollutants concentrations.[41,43,44] In our case, the production rate of H_2O_2 with respect to the initial dye concentration, which is integrated in Figure 6, supports the above explanation.

2.5. Effect of initial pH

In water and wastewater treatment, pH is a crucial parameter. It affects the chemical structures of the organic pollutants and their reactivity. In order to study the influence of the initial pH of the solution during the ultrasonic degradation of BR29 (30 mg L^{-1}), four different pH values were chosen: pH 3.0, natural pH (5.6), pH 8.2, and pH 10.1. The obtained results are depicted in Figure 7. It can be observed from this figure that the degradation of BR29 was faster at an acidic pH and much slower at alkaline pH conditions. The difference in degradation rates between pH levels of 3.0 and 5.6 is relatively highly consistent with the findings of Ferkous et al.[43] during the sonochemical degradation of naphthol blue black dye at 585 kHz. It was, however, nonsignificant between natural and alkaline pH levels. This is consistent with the report of Ince and Tezcanli-Guyer concerning the sonochemical degradation of two aryl-azo-naphthol dyes at 300 kHz.[45] The initial degradation rate of BR29 was increased by a factor of 1.65 when the pH solution was decreased from 10.1 to 3.0 (Figure 7, the insert).

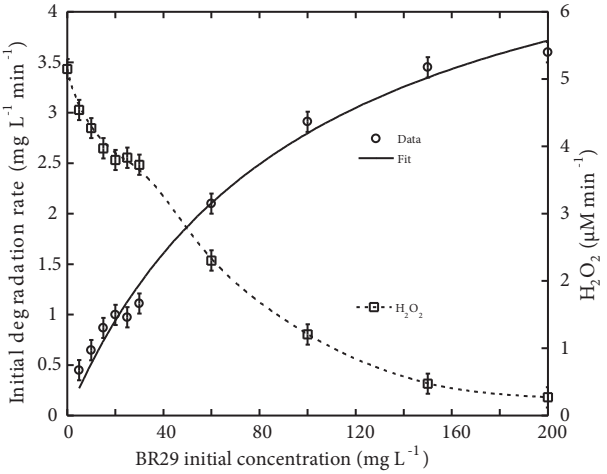

Figure 6. Initial degradation rate and H_2O_2 production rate as a function of initial concentration of BR29, for the same conditions as in Figure 5.

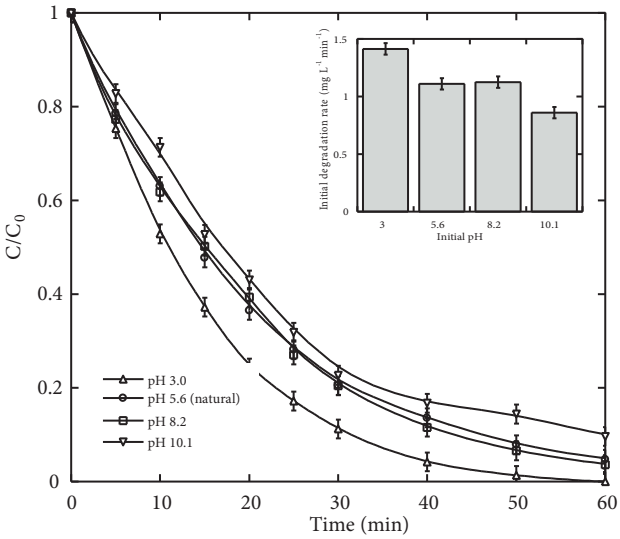

Figure 7. Effect of initial solution pH on the sonochemical degradation of BR29 (conditions – volume: 300 mL, initial dye concentration (C_0): 30 mg L^{-1}, temperature: 25 ± 2 °C, pH 3.0–10.1, frequency: 300 kHz, power: 80 W).

The determination of the limit of the protonated and ionized form of BR29 is not possible due to the lack of its dissociation constant (pKa). However, based on the obtained results (Figure 7), it can be suggested that the fraction of the hydrophilic ionized form was increased with pH rise. At pH 3.0, a high fraction of BR29 in its hydrophobic protonated form accumulates at the bubble/solution interface, thereby resulting in a higher degradation rate. However, a higher pH favors a more ionized fraction of the dye, thereby enhancing its hydrophilic nature and allowing degradation to take place in the bulk of the solution where a lower amount of hydroxyl radicals can arrive before recombination.

2.6. Effect of power intensity

The acoustic powers dissipated into the solution, estimated using the standard calorimetric method,[46] were found to be ∼50% of the electrical delivered powers. The acoustic amplitude P_A is directly related to the power intensity I_a, or acoustic power per unit area, as $P_A = (2I_a\rho_L c)^{1/2}$.

The effect of power intensity in the range of 0.8–3.2 W cm^{-2} on the sonolytic degradation of BR29 (30 mg L^{-1}) was investigated and the obtained results are depicted in Figure 8. As can be seen, the higher the delivered power, the higher was the degradation rate of the dye. The initial degradation rate increased from 0.318 mg L^{-1} min^{-1} at 0.8 W cm^{-2} to 0.566, 0.992, and 1.110 mg L^{-1} min^{-1} for, respectively, 1.6, 2.4, and 3.2 W cm^{-2}. Similar results were reported by Torres-Palma et al.,[27] Moumeni et al.,[47] and Ferkous et al.[48]

With an increase in acoustic amplitude, the bubble will reach higher R_{max} and lower R_{min} with a higher amount of water vapor being trapped in the bubble at the collapse (R_{max} and R_{min} are, respectively, the maximum and the minimum bubble radii attained during oscillation).[49] This results in stronger implosions with higher bubble core temperatures and pressures at the final stage of the bubble collapse, and with the higher water vapor trapped at this moment, higher amounts of hydroxyl radical will be generated since it results principally from the dissociation of water vapor molecules inside the bubble. Moreover, it has recently

been reported that the acoustic amplitude affects the range of ambient bubble radius for the production of $HO^{\bullet}$ radical and the higher the acoustic amplitude was, the higher was the range of active bubbles for the production of the oxidants.[39] This implies that higher acoustic amplitude yields a higher number of bubbles and this leads to a higher concentration of $^{\bullet}OH$ radicals in the dye solution. Consequently, the results of an increase in power intensity are greater sonochemical effects on microscopic and macroscopic scales (bubble and solution, respectively), resulting in higher BR29 degradation rates.

2.7. Effect of the nature of dissolved gas

The effect of argon, air, and nitrogen as saturating gases on the sonochemical degradation of BR29 (30 mg L^{-1}) was investigated. In each experiment, the gas was bubbled 20 min prior to starting and until completion of experiments. The obtained results are plotted in Figure 9. As observed, the degradation rate followed the order of Ar > air > control > N_2. Ar provided complete removal after 60 min of sonication with an initial degradation rate of 1.876 mg L^{-1} min^{-1}. The percentage of BR29 removed decreases to 97% and 89% with initial rates of 1.335 and 0.901 mg L^{-1} min^{-1} for air and N_2, respectively. These results are in good agreement with that reported in the case of several nonvolatile organic pollutants.[27,43,44]

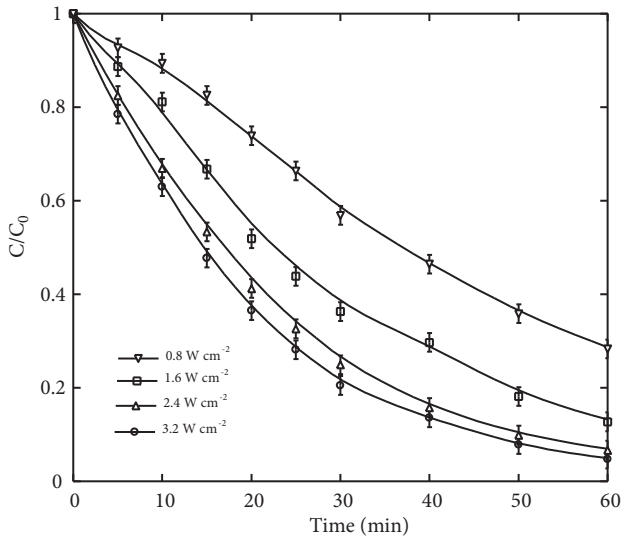

Figure 8. Effect of power intensity on the sonochemical degradation of BR29 (conditions – volume: 300 mL, initial dye concentration (C_0): 30 mg L^{-1}, temperature: 25 ± 2 °C, pH ∼5.6, frequency: 300 kHz).

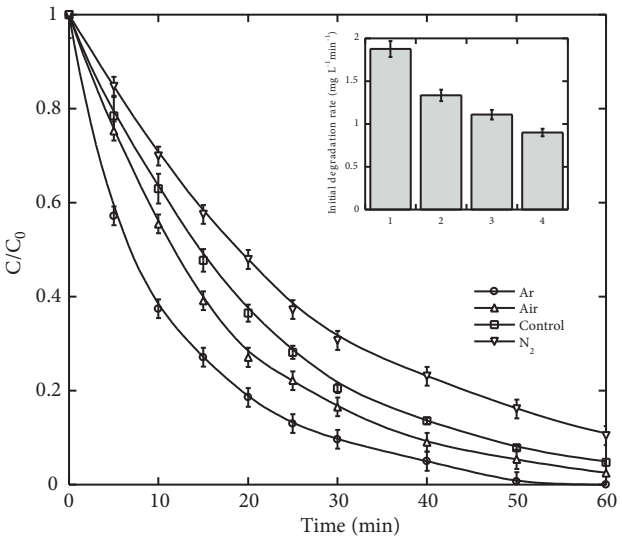

Figure 9. Effect of the nature of dissolved gas on the sonochemical degradation of BR29 (conditions – volume: 300 mL, initial BR29 concentration (C_0): 30 mg L^{-1}, temperature: 25 ± 2 °C, pH ∼5.6, frequency: 300 kHz, ultrasonic power: 80 W).

Dissolved gases influence sonolysis through three aspects.[50] First, monatomic gases typically have greater polytropic indexes γ ($\gamma = c_p/c_v$) than polyatomic gases, and the higher polytropic index results in higher temperature achieved in the bubble at collapse. Second, gases with low thermal conductivities can reduce the heat dissipation, thus facilitating the increase in collapse temperatures and enhancing sonochemical reactivity. Third, gas with higher solubility can create more nucleation sites and improve the cavitation events. In this study, argon has a greater polytropic ratio ($\gamma_{Ar} = 1.66$) and solubility ($x_{Ar} = 2.748 \times 10^{-5}$)[51] and lower

thermal conductivity (λ_{Ar} = 0.018 W m^{-2} K^{-1})[52] than air and N_2 gases, which have the same γ and λ (γ = 1.41, λ = 0.026 W m^{-2} K^{-1})[52] and a slight difference in their solubility (x_{air} = 1.524 × 10^{-5}, x_{N2} = 1.276 × 10^{-5}).[51] Therefore, it achieved the highest degradation rate as it could generate a higher bubble yield ($HO^{\bullet}$ radical) and greater number of bubbles. However, the beneficial effect of air compared to N_2 was mainly attributed to the internal bubble chemistry. In our recent paper,[31] a detailed numerical investigation of the effect of nature of dissolved gas on single bubble sonochemistry was carried out. It was found that the production rate of $HO^{\bullet}$ radical from the collapsing bubble is strongly dependent on the trapped amount of N_2 gas at collapse, and the higher the concentration of N_2, the lower will be the production rate of $HO^{\bullet}$ radical.[31] This trend was associated with the consumption of $^{\bullet}OH$ radical through the reaction NO + $HO^{\bullet}$ + M $\leftrightarrow$ HNO_2 + M. Because oxidizing nitrogen NO is formed mainly, as found, through the reactions N_2 + O = NO + N and NO_2 + M = O + NO + M, the higher the concentration of N_2 in the bubble, the higher will be the concentration of NO and this accelerates the consumption rate of $^{\bullet}OH$ radical through the reaction NO + $HO^{\bullet}$ + M = HNO_2 + M.

2.8. Effect of environmental matrices

Salts and natural organic matter (NOM) existing in natural waters are potential inhibitors for several advanced oxidation processes, i.e. Fenton,[53] UV/H_2O_2,[54] and UV/O_3.[55] To verify the impact of the presence of salts and NOM on the sonochemical treatment, degradation experiments (300 kHz, 80 W, and 30 mg L^{-1} BR29) were conducted in different environmental matrices, namely natural mineral water, seawater, and river water, at a natural pH. The principle characteristics of mineral water and seawater used in this study are summarized in Table 1. The river water (pH ~7.7) automatically contains salts and NOM (principally humic and fulvic acids) with unknown concentrations. The results of the degradation kinetics are shown in Figure 10. As can be observed, the natural aqueous matrices significantly enhanced the ultrasonic degradation of the dye. The best conversion rate was observed for natural mineral water, followed by river water and then seawater. Sanchez-Prado et al.[56] studied the sonochemical degradation of triclosan in water and wastewater and reported a beneficial effect of seawater and then urban runoff water on the degradation rate compared to that observed with deionized water. Taking into account that solution pH in the range of 5.6–8.2 has no impact on the sonochemical degradation of BR29 (Figure 7), the observed beneficial effect of natural water was completely attributed to the salting-out effect on both the pollutant and the dissolved gas as well as the inhibition of the bubble coalescence.[57] Under the rise of ionic strength induced by the presence of salts, the solute is expected to migrate from bulk solution to the interface of the bubble/solution where the concentration of hydroxyl radicals is high and degradation is likely to occur fast.[58] Simultaneously, the presence of salts reduces the amount of dissolved gas, and hence the bubble coalescence will also be reduced, resulting in a greater number of small bubbles of higher sonochemical activity.[37] However, the lower positive effect of seawater compared to those of mineral and river waters was attributed to the ultrasound attenuation due to the high solution viscosity and surface tension induced by the high quantity of salts presents in seawater. Sonochemical degradation (initial rate) in river water was about 1.4 times as fast as that in deionized water. This can be explained, in addition to the salting-out effect, by the dissolved solids facilitating bubble nucleation. Keck et al.,[59] who investigated the sonochemical degradation of various aromatics in the presence and absence of inert quartz particles in the range 2–25 μm, reported that performance was enhanced in the presence of solids and this was ascribed to solids altering the shape of bubbles from spherical to asymmetric, thus yielding larger surfaces available to react with more solute molecules.

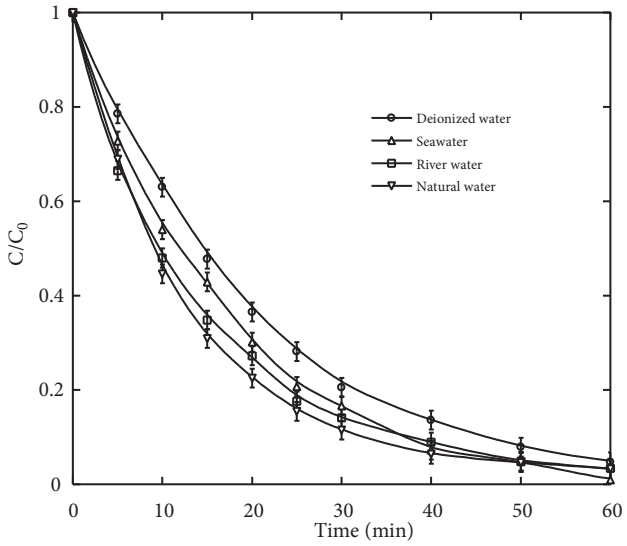

Figure 10. Sonochemical treatment of BR29 in seawater, river water, and natural water (conditions – volume: 300 mL, initial BR29 concentration (C_0): 30 mg L^{-1}, temperature: 25 ± 2 °C, natural pH, frequency: 300 kHz, ultrasonic power: 80 W).

Table 1. Principal characteristics of mineral water and seawater used in this study.

	Mineral water	Seawater
pH	7	7.5
Ca^{2+}	59.0 mg L^{-1}	0.4 g L^{-1}
Mg^{2+}	45.0 mg L^{-1}	1.3 g L^{-1}
Na^{+}	15.0 mg L^{-1}	11.0 g L^{-1}
K^{+}	2.0 mg L^{-1}	-
Cl^{-}	22.0 mg L^{-1}	20.0 g L^{-1}
SO_4^{2-}	40.0 mg L^{-1}	3.0 g L^{-1}
HCO_3^{-}	378.2 mg L^{-1}	-

2.9. Oxidation/mineralization and improvement methods

Although 300-kHz ultrasonic waves were efficient for the removal of BR29, it was of interest to evaluate the action of this technique on the degree of oxidation and mineralization of the dye solution. Experiments were conducted at 300 kHz and 80 W with 30 mg L^{-1} of BR29 and natural pH to evaluate the COD and total organic carbon (TOC) removal during the sonochemical treatment. The results of these experiments are presented in Figure 11. As can be observed, while BR29 was eliminated after 120 min, only 7% of TOC and 27% of COD were removed, and after a long irradiation time (240 min) the TOC and COD abatement was 15% and 28%, respectively. These results are in good agreement with that obtained by Torres-Palma et al.[60] for the degradation of bisphenol A at the same sonochemical parameters (300 kHz, 80 W). Villegas-Guzman et al.[61] also reported a lower TOC and COD (∼5% and ∼20%, respectively) after 200 min of irradiation at 600 kHz and 60 W of an aerated solution of dicloxacillin (0.211 mM). The low conversion of TOC and COD obtained confirms that the action of ultrasound on nonvolatile organic pollutants leads to very hydrophilic intermediates, which are less likely to approach the cavity/liquid interface where the concentration of hydroxyl radical is predominant. In fact, an estimated 80% of the radicals generated by sonolysis recombine, and only a small amount of $HO^{\bullet}$ radicals escape and react

with organic molecules in solution.[62] This implies that the probability of these products for making contact with $HO^{\bullet}$ radicals is very low, yielding a low degree of mineralization.

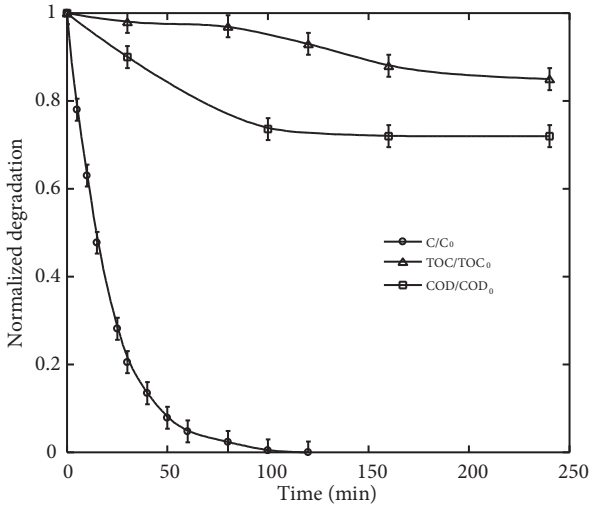

Figure 11. Total organic carbon (TOC) and chemical oxygen demand (COD) abatements under ultrasound treatment of aerated BR29 solution (conditions – volume: 300 mL, initial BR29 concentration (C_0): 30 mg L^{-1}, temperature: 25 ± 2 °C, pH ~5.6, frequency: 300 kHz, power: 80 W).

One of the solutions proposed to overcome the weakness of ultrasound toward TOC removal is the assistance of ultrasonic treatment with a low amount of iron, i.e. Fe^{2+}. In this case, the ultrasonically generated H_2O_2 in the presence of substrate decomposes via Fenton reaction (Eqs. (8)–(11)), yielding an excess of $^{\bullet}OH$ radicals in the bulk solution.[60]

$$Fe^{2+} + H_2O_2 \rightarrow Fe^{3+} + OH^- + HO^{\bullet} \tag{8}$$

$$Fe^{3+} + H_2O_2 = Fe - OOH^{2+} + H^+ \tag{9}$$

$$Fe - OOH^{2+} \rightarrow Fe^{2+} + HO_2^{\bullet} \tag{10}$$

$$Fe^{3+} + HO_2^{\bullet} \rightarrow Fe^{2+} + O_2 + H^+ \tag{11}$$

For verifying this hypothesis, the sonochemical (300 kHz, 80 W) mineralization of BR29 (30 mg L^{-1}) was evaluated in the presence of 15 mg L^{-1} of Fe^{2+} at pH 3, to avoid Fe^{2+} precipitation as iron hydroxide (the amount of iron is optimized). The obtained results are summarized in Table 2 at various reaction times. It was observed that the mineralization and oxidation of the dye was distinctly increased in the presence of Fe^{2+}. The TOC removal increased from 2.5% with ultrasound alone to 35% with the ultrasound/Fe^{2+} system after 30 min of treatment and from 5% with ultrasound to 50% with the ultrasound/Fe^{2+} process after 1 h of treatment. Similarly, the COD abatement increased from 27% with ultrasound to 83% with the ultrasound/Fe^{2+} system after 100 min of sonication. This is due to the Fe^{2+} playing the role of catalyst and initiating the decomposition of the sonochemically yielded H_2O_2 to generate an excess of $HO^{\bullet}$ radical in the bulk solution.[60] The H_2O_2

accumulation rate in the presence of BR29 (30 mg L^{-1}) was measured and found to be 4.53 μM min^{-1}. All these findings are consistent with those reported by Torres-Palma et al.[60] for the degradation of bisphenol A at the same sonochemical parameters, but for 7 mg L^{-1} of Fe^{2+}.

Table 2. TOC and COD removal during the sonochemical degradation of BR29 in the presence of 15 mg L^{-1} of Fe^{2+} (conditions – volume: 300 mL, initial BR29 concentration: 30 mg L^{-1}, COD_0 = 46.08 mg L^{-1}, TOC_0 = 5.80 mg L^{-1}, temperature: 25 ± 2 °C, pH ~3, frequency: 300 kHz, power: 80 W).

Time (min)	TOC removal (%)	COD removal (%)
0	0.0	0.0
30	31.0	81.3
60	50.0	83.5
100	51.0	85.3

3. Experimental

3.1. Reagents

Basic Red 29 (abbreviation: BR29; CAS number: 42373-04-6; molecular formula: $C_{19}H_{17}ClN_4S$, molecular weight: 368.88 g mol^{-1}) was supplied by Sigma-Aldrich and used without any purification.

Potassium iodide, sodium hydroxide, sulfuric acid, ammonium heptamolybdate $(NH_4)_6Mo_7O_{24}.4H_2O$, tert-butyl alcohol, and glucose (all from Sigma-Aldrich) were used as received (analytical grade).

3.2. Ultrasonic reactor

Sonolysis experiments were conducted in a cylindrical water-jacketed glass reactor. The ultrasonic waves of 300 kHz were emitted in continuous mode from the bottom of the reactor through a piezoelectric disk (diameter: 4 cm) fixed on a Pyrex plate (diameter: 5 cm). The emitting system was connected to a high-frequency generator operating at variable supplied power. The temperature of the solution was monitored using a thermocouple immersed in the reacting medium.

3.3. Procedures

All BR29 solutions were prepared with distilled water. Experiments of BR29 degradation were carried out under different conditions using a constant solution volume of 300 mL. The pH of the solution was adjusted using NaOH or H_2SO_4. The temperature of the sonicated solution was kept constant at 25 ± 2 °C by circulating cooling water through a jacket surrounding the cell. Aqueous samples were taken periodically from the solution and the concentrations of the dye were determined using a UV-Vis spectrophotometer (Lightwave II). All experiments were conducted at least in triplicate, and the data were averaged.

Hydrogen peroxide concentration during water sonolysis was analytically determined using the iodometric method.[63] Sample aliquots taken periodically from the reactor during sonolysis were added to the quartz cell of the spectrophotometer containing 1 mL of potassium iodide (0.1 M) and 20 μL of ammonium heptamolybdate (0.01 M). The iodide ion (I^-) reacts with H_2O_2 to form the triiodide ion (I_3^-). The mixed solutions were allowed to stand for 5 min before absorbance was measured. The absorbance was recorded with a UV-Vis spectrophotometer (Lightwave II) at the maximum wavelength of the formed triiodide (I_3^-) (352 nm; molar absorptivity = 26300 L mol^{-1} cm^{-1}).

A MembraPure uniTOC lab analyzer was used for TOC measurements. The instrument, equipped with an automatic sample injector, uses UV/persulfate oxidation followed by CO_2-selective highly sensitive nondispersive infrared detection.

COD was measured according to the method presented by Thomas and Mazas,[64] using a dichromate solution (Sigma-Aldrich) as the oxidizer in a strong acid medium. The test solution (2 mL) was transferred into the dichromate reagent and digested at 150 °C for 2 h. The optical density for the color change of dichromate solution was determined spectrophotometrically at 440 nm.

4. Conclusion

The sonochemical process using high-frequency ultrasound (300 kHz) offers a valuable alternative for the degradation of BR29 dye in aqueous solutions, particularly those containing various matrix components such as salts and NOM, which are potential inhibitors for several advanced oxidation techniques. Radical scavenger tests with tert-butyl alcohol and glucose revealed that the $HO^{\bullet}$ radical was responsible for the degradation of BR29. The production rate of $HO^{\bullet}$ radical was estimated to be 8.76 μM min^{-1} at 300 kHz and 3.2 W cm^{-2}. Numerical simulations of bubble oscillation under the experimental conditions confirmed the formation of the hydroxyl radical, which attained its upper concentration at the end of the bubble collapse. The degradation rate increased with increasing initial BR29 concentration in the range of 5–200 mg L^{-1}, following a Langmuir-type kinetics model. The results showed that fast degradation occurred at an initial pH of 3.0. The sonochemical degradation rate was more efficient at higher power intensities. The degradation rate was faster in environmental matrices than deionized water. The best conversion was observed for natural water, followed by river water and then seawater. Although low degrees of mineralization and oxidation were obtained with ultrasound alone ($\sim$7% of TOC and $\sim$20% of COD), an improvement method based on the addition of low iron quantity into the sonicating solution allows us to overcome this problem. The sono-Fenton process increased the TOC removal to 50% and the COD elimination to 83% in only 1 h of treatment.

Acknowledgment

Financial support by the Ministry of Higher Education and Scientific Research of Algeria (Project No. A16N01UN230120130010) is gratefully acknowledged.

References

1. Wang, Z.; Xue, M.; Huang, K.; Liu, Z. In *Advances in Treating Textile Effluent*; Hauser, P., Ed. InTech: Rijeka, Croatia, 2011, pp. 91–116.
2. Przystaś, W.; Zabłocka-Godlewska, E.; Grabińska-Sota, E. *Water Air Soil Pollut.* **2012**, *223*, 1581-1592.
3. Pereira, L.; Alves, M. In *Environmental Protection Strategies for Sustainable Development, Strategies for Sustainability*; Malik, A.; Grohmann, E., Eds. Springer: London, UK, 2012, pp. 111-162.
4. Zaharia, C.; Suteu, D. In *Organic Pollutants Ten Years after the Stockholm Convention - Environmental And Analytical Update*; Puzyn, T., Ed. InTech: Rijeka, Croatia, 2012, pp. 55-86.
5. Brown, M. A.; De Vito, S. C. *Crit. Rev. Env. Sci. Technol.* **1993**, *23*, 249-324.
6. Arslan, M.; Sayin, S.; Yilmaz, M. *Water Air Soil Pollut.* **2013**, *224*, 1527-1536.
7. Latif, A.; Noor, S.; Sharif, Q. M.; Najeebullah, M. *J. Chem. Soc. Pak.* **2010**, *32*, 115-124.
8. Robinson, T.; McMullan, G.; Marchant, R.; Nigam, P. *Bioresour. Technol.* **2001**, *77*, 247-255.
9. Choi, Y.; Park, B.; Cha, D. K. *Korean J. Chem. Eng.* **2015**, *32*, 1812-1817.

10. Zabłocka-Godlewska, E.; Przystaś, W.; Grabińska-Sota, E. *Water Air Soil Pollut.* **2014**, *225*, 1846.
11. Lee, H. J.; Kang, D. W.; Chi, J.; Lee, D. H. *Korean J. Chem. Eng.* **2003**, *20*, 503-508.
12. Wang, J. L.; Xu, L. J. *Crit. Rev. Env. Sci. Technol.* **2012**, *42*, 251-325.
13. Parsons, S. *Advanced Oxidation Processes for Water and Wastewater Treatment*; IWA Publishing: London, UK, 2004.
14. Hunsberger, J. F. In *Handbook of Chemistry and Physics*; Weast, R. C., Ed. CRC Press: Boca Raton, FL, USA, 1977, pp. D141-144.
15. Tarr, M. A. *Chemical Degradation Methods for Wastes and Pollutants*; Marcel Dekker: New York, NY, USA, 2003.
16. Park, J. Y.; Lee, I. H. *Korean J. Chem. Eng.* **2009**, *26*, 387-391.
17. Adewuyi, Y. G. *Ind. Eng. Chem. Res.* **2001**, *40*, 4681-4715.
18. Kim, I.; Yoa, S. J.; Lee, J. K.; Huang, C. P. *Korean J. Chem. Eng.* **2003**, *20*, 1045-1053.
19. Suslick, K. S.; Didenko, Y.; Fang, M. M.; Hyeon, T.; Kolbeck, K. J.; McNamara, W. B.; Mdleleni, M. M.; Wong, M. M. *Philos. T. Roy. Soc. A* **1999**, *357*, 335-353.
20. Suslick, K. S.; Flannigan, D. J. *Annu. Rev. Phys. Chem.* **2008**, *59*, 659-683.
21. Makino, K.; Mossoba, M. M.; Riesz, P. *J. Am. Chem. Soc.* **1982**, *104*, 3537-3539.
22. Castellanos, M. M.; Reyman, D.; Sieiro, C. *Ultrason. Sonochem.* **2001**, *8*, 17-22.
23. Thompson, L. H.; Doraiswamy, L. K. *Ind. Eng. Chem. Res.* **1999**, *38*, 1215-1249.
24. Pétrier, C.; Francony, A. *Ultrason. Sonochem.* **1997**, *4*, 295-300.
25. Putterman, S. J.; Weninger, K. R. *Annu. Rev. Fluid Mech.* **2000**, *32*, 445-476.
26. Buxton, G. V.; Greenstock, C. L.; Helman, W. P.; Ross, A. B. *J. Phys. Chem. Ref. Data* **1988**, *17*, 515.
27. Torres-Palma, R. A.; Pétrier, C.; Combet, E.; Carrier M.; Pulgarin, C. *Ultrason. Sonochem.* **2008**, *15*, 605-611.
28. Merouani, S.; Hamdaoui, O.; Rezgui, Y.; Guemini, M. *Acta Acust. United Acust.* **2014**, *100*, 823-833.
29. Merouani, S.; Hamdaoui, O.; Rezgui, Y.; Guemini, M. *Ultrason. Sonochem.* **2014**, *21*, 53-59.
30. Merouani, S.; Hamdaoui, O.; Rezgui, Y.; Guemini, M. *Ultrason. Sonochem.* **2015**, *22*, 41-50.
31. Merouani, S.; Hamdaoui, O.; Rezgui, Y.; Guemini, M. *Ultrason. Sonochem.* **2015**, *22*, 51-58.
32. Tauber, A.; Mark , G.; Shuchmann, H. P.; Von Sonntag, C. *J. Chem. Soc. Perkin Trans.* **1999**, *2*, 1129-1135.
33. Wayment, D. G.; Casadonte, D. J. *Ultrason. Sonochem.* **2002**, *9*, 251-257.
34. Merouani, S.; Hamdaoui, O.; Saoudi, F.; Chiha, M.; Pétrier, C. *J. Hazard. Mat.* **2010**, *175*, 593-599.
35. Iida, Y.; Yasui, K.; Tuziuti, T.; Sivakumar, M. *Microchem. J.* **2005**, *80*, 159-164.
36. Merouani, S.; Hamdaoui, O.; Saoudi, F.; Chiha, M. *J. Hazard. Mater.* **2010**, *187*, 1007-1014.
37. Brotchie, A.; Statham, T.; Zhou, M.; Dharmarathane, L.; Grieser, F.; Ashokkumar, M. *Langmuir* **2010**, *26*, 12690-12695.
38. Labouret, S.; Frohly, J. *10 ème Congrès Français d'Acoustique*; Lyon, France, 2010 (in French).
39. Merouani, S.; Hamdaoui, O.; Rezgui, Y.; Guemini, M. *Ultrason. Sonochem.* **2013**, *20*, 815-819.
40. Okitsu, K.; Iwasaki, K.; Yobiko, Y.; Bandow, H.; Nishimura, R.; Maeda, Y. *Ultrason. Sonochem.* **2005**, *12*, 255-262.
41. Gao, Y. Q.; Gao, N. Y.; Deng, Y.; Gu, J. S.; Gu, Y. L.; Zhang, D. *Ultrason. Sonochem.* **2013**, *20*, 1401-1407.
42. Villaroel, E.; Silva-Agredo, J.; Petrier, C.; Taborda, G.; Torres-Palma, R. A. *Ultrason. Sonochem.* **2014**, *21*, 1763-1772.
43. Ferkous, H.; Hamdaoui, O.; Merouani, S. *Ultrason. Sonochem.* **2015**, *26*, 30-39.
44. Guzman-Duque, F.; Pétrier, C.; Pulgarin, C.; Peñuel, G.; Torres-Palma, R. A. *Ultrason. Sonochem.* **2011**, *18*, 440-446.

45. Ince, N. H.; Tezcanali-Guyer, G. *Ultrasonics* **2004**, *42*, 591-596.
46. Mason, T. J.; Lorimer, J. P.; Bates, D. M. *Ultrasonics* **1992**, *30*, 40-42.
47. Moumeni, O.; Hamdaoui, O.; Pétrier, C. *Chem. Eng. Process.* **2012**, *62*, 47-53.
48. Ferkous, H.; Merouani, S.; Hamdaoui, O.; Rezgui, Y.; Guemini, M. *Ultrason. Sonochem.* **2015**, *26*, 30-39.
49. Merouani, S.; Hamdaoui, O.; Rezgui, Y.; Guemini, M. *Res. Chem. Intermed.* **2015**, *41*, 881-897.
50. Rooze, J., Rebrov, E. V.; Schouten, J. C; Keurentjes, J. T. F. *Ultrason. Sonochem.* **2013**, *20*, 1-11.
51. Fogg, P. G. T.; Gerrard, W. *Solubility of Gases in Liquids*; John Wiley & Sons: Chichester, UK, 1990.
52. Beaton, C. F.; Hewitt, G. F. *Physical Property Data for the Design Engineer*; Hemisphere Publishing Corporation: New York, NY, USA, 1989.
53. Torres-Palma, R. A.; Abdelmalek, F.; Combet, E.; Pétrier, C.; Pulgarin, C. *J. Hazard. Mat.* **2007**, *146*, 546-551.
54. Guittonneau, S.; De Laat, J.; Dore, M.; Duguet, J. P.; Honnel C. *Rev. Sc. Eau* **1988**, *1*, 35-54.
55. Tanaka, T.; Tsuzuki K.; Takagi, T. *Water Sci. Technol.* **2001**, *43*, 295-302.
56. Sanchez-Prado, L.; Barro, R.; Garcia-Jares, C.; Llompart, M.; Lores, M.; Petrakis, C.; Kalogerakis, N.; Mantzavinos, D.; Psillakis, E. *Ultrason. Sonochem.* **2008**, *15*, 689-694.
57. Ferkous, H.; Merouani, S.; Hamdaoui, O. *J. Water Process. Eng.* **2016**, *9*, 67-77.
58. Seymour, J. D.; Gupta, R. B. *Ind. Eng. Chem. Res.* **1997**, *36*, 3453-3457.
59. Keck, A.; Gilbert E.; Köster, R. *Ultrasonics* **2002**, *40*, 661-665.
60. Torres-Palma, R. A.; Pétrier, C.; Combet, E.; Moulet, F.; Pulgarin, C. *Environ. Sci. Technol.* **2007**, *41*, 297-302.
61. Villegas-Guzman, P.; Silva-Agredo, J.; Giraldo-Aguirre, A. L.; Flórez-Acosta, O.; Petrier, C.; Torres-Palma, R. A. *Ultrason. Sonochem.* **2015**, *22*, 211-219.
62. Dalhatou, S.; Pétrier, C.; Laminsi, S.; Baup, S. *Int. J. Environ. Sci. Technol.* **2015**, *12*, 35-44.
63. Kormann, C.; Bahnemann, D. W.; Hoffmann, M. R. *Environ. Sci. Technol.* **1988**, *22*, 798-806.
64. Thomas, O.; Mazas, N. *Analusis* **1986**, *14*, 300-302.